Hydrogeology Journal (2019) 27:717–730
https://doi.org/10.1007/s10040-018-1889-9

PAPER

Regional groundwater flow system in a stratovolcano adjacent to a coastal area: a case study of Mt. Fuji and Suruga Bay, Japan

Masahiko Ono[1] · Isao Machida[1] · Reo Ikawa[1] · Takafumi Kamitani[2] · Koichi Oyama[3] · Yasuhide Muranaka[2] · Akira Ito[4] · Atsunao Marui[1]

Received: 24 April 2018 / Accepted: 24 October 2018 / Published online: 20 November 2018

Abstract

Groundwater movement through the slope area of Mt. Fuji to the coastal area of Suruga Bay (central Japan) was investigated using spatially dense geochemical data, as a case study for elucidating the groundwater flow system in a stratovolcano adjacent to the coast. Spatial distributions of the hydrogen stable isotope ratio, vanadium concentration, and water temperature in the groundwater showed anomalies at the coastal area of Suruga Bay. The anomalies were characterized as depleted isotope ratio, high vanadium concentration, and low water temperature relative to surroundings. This can be explained as a regional deep groundwater flow from the slope of Mr. Fuji to the coastal area of Suruga Bay because groundwater recharged at higher elevation has a depleted isotope ratio caused by the altitude effect and high vanadium concentration as a result of dissolution from the basaltic aquifer. These characteristics also imply a hierarchical flow system, which is incorporated into a hydrogeological model of the coastal aquifer.

Keywords Groundwater flow · Volcano · Coastal area · Stable isotopes · Japan

Introduction

Groundwater is a valuable water resource in volcanic regions, especially volcanic islands, and has been used for domestic, agricultural, and industrial purposes (Meinzer 1930; Stern and Macdonald 1947; D'Alessandro and Vita 2003). Meanwhile, as volcanic islands are surrounded by the sea and many volcanoes are found in coastal areas, the threat of saltwater intrusion into the coastal aquifer, caused by over pumping of groundwater resources, is ever-present. Although the numerical modeling of groundwater flow at basin scale is one of the tools needed for effective water resource management, it is sometimes difficult to construct due to a heterogeneous and anisotropic geological structure, masked geomorphological properties by an overlap of younger deposit, and scarce hydrogeological information in the deep zone associated with the difficulty of deep-well drilling, and so on.

There is a long history of international hydrogeological research into volcanoes. From geological exploration on the basaltic island of Tenerife in the Spanish Canary Islands, Ecker (1976) determined the occurrence of aquifers formed by compartments (voids) and secondary fractures. Mink (1976) showed the hydrogeological cross sections in Guam (Western Pacific), in which all the exploitable groundwater occurs in the permeable limestone while volcanic rock plays the role of hydraulic basement. Macdonald et al. (1983) showed that the occurrence of groundwater on the Hawaiian island of Oahu (Central Pacific) is characterized by the presence of basal groundwater, perched groundwater, and dyke-impounded groundwater; and that the discontinuity of these groundwater types is responsible for the occurrence of high-

Electronic supplementary material The online version of this article (https://doi.org/10.1007/s10040-018-1889-9) contains supplementary material, which is available to authorized users.

✉ Masahiko Ono
masa.ono@aist.go.jp

[1] Geological Survey of Japan, National Institute of Advanced Industrial Science and Technology (AIST), Central 7, 1-1-1 Higashi, Tsukuba, Ibaraki 305-8567, Japan

[2] Shizuoka Institute of Environment and Hygiene, 4-27-2 Kita-ando, Aoi-ku, Shizuoka 420-8637, Japan

[3] Administrative Bureau, Numazu Public Works Office, 1-3 Takashima-Honchou, Numazu 410-0055, Japan

[4] Living Environment Division, Shizuoka Prefectural Government, 9-6 Ote-machi, Aoi-Ku, Shizuoka 420-8601, Japan

level groundwater in the island. Similar classifications were reported in Jeju Island, Korea (Won et al. 2006) and in Madeira Island, Portugal (Prada et al. 2005).

The aforementioned studies are very important for obtaining an image of groundwater occurrence in a volcano accompanied by complicated geological structure. To connect such knowledge about groundwater occurrence to numerical models of groundwater flow, geochemical investigation is necessary to understand the flow paths and groundwater age in a volcano. From that perspective, Custodio (1989) summarized how to use environmental isotope techniques to obtain such characteristics in volcanic formations. The techniques have been widely applied in many volcanic regions (e.g. Scholl et al. 1996; Hildenbrand et al. 2005; Herrera and Custodio 2008; Asai et al. 2009; Heilweil et al. 2009). The research findings suggested that a conceptual model can be improved by combining hydrogeological information with geochemical data on natural water. Knowledge about groundwater flow models in volcanic regions has been accumulated steadily to conduct more precise numerical modeling of groundwater flow for effective water resource management; thus, knowledge of groundwater flow that is verified by spatially dense geochemical data should be accumulated—for example, Kebede et al. (2008) constructed a conceptual model of groundwater flow in the Ethiopian rift volcanic aquifers based on a large number of geochemical data. Parisi et al. (2011) showed the conceptual model of groundwater flow in Mt. Vulture, southern Italy, which was elucidated by the geochemical investigation for groundwater from horizontal and vertical wells. These models will help in validating a numerical model of groundwater flow more precisely.

From that perspective, Mount Fuji volcano, the highest mountain in Japan, was selected as the study area. The geology in the study area is composed of permeable volcanic and alluvial fan deposits and the area is surrounded by the Suruga Bay and an influent river, implying the presence of complicated boundary conditions. It is expected that a geochemical study can demonstrate a groundwater flow system by using a large number of groundwater samples taken from shallow and deep wells. In addition, it is also well known that this area produces abundant and good-quality water, being representative of the rich groundwater resources in Japan. Therefore, the present study can be regarded as an example of features that lead to groundwater abundance at the foot of a volcano. The present study clarifies the groundwater flow system of the volcano including the coastal area with a revision of an existing groundwater flow model by using isotopes, water quality, and water temperature in the groundwater. This paper also describes knowledge of a hierarchical flow system in the stratovolcano, which will assist hydrogeological modeling in this area and other volcanic regions.

Materials and methods

Hydrogeology of Mt. Fuji

The study area is located in the southwestern area of Mt. Fuji, Japan (Fig. 1a). Mt. Fuji is a stratovolcano with an elevation of 3,773 m above mean sea level (amsl) at the summit. Annual rainfall at four observatories (Mishima, Fuji, Furuseki, and Yamanaka) around Mt. Fuji ranged from 1,600 to 2,100 mm for 1981–2010 (Japan Meteorological Agency 2015). Kizawa et al. (1969) reported that the rainfall amount at the summit of Mt. Fuji was approximately 1.5 times greater than at the foot area. Yamamoto (1970) suggested that the total amount of groundwater recharge in the Mt. Fuji area is approximately 2.2 billion m^3/year and proposed that the hydrological structure of the region could be grouped into three zones: an "upper recharging zone" (from the summit to 2,000 m amsl), a "middle recharging zone" (2,000–1,000 m amsl), and a "spring zone" (below 1,000 m amsl). There are five lakes in the north of Mt. Fuji, referred to as the "Fuji-Goko Lakes", and groundwater discharge from the bottom of one of these lakes has been observed (Marui et al. 1995).

Figure 1b shows the generalized groundwater flow system and a geological model of Mt. Fuji. The Tertiary layer (Misaka Mountains) underlies Mt. Fuji and is covered by the Komitake volcano, Ko-Fuji volcano, and ejecta of the younger Fuji (Tsuya 1940). The ejecta of the younger Fuji forms a highly permeable layer, distributed in concentric circles around the present summit (Kurata 1966), and numerous springs emerge at the edge of the layer; the layer of younger Fuji ejecta has been recognized as a potential aquifer in this region. In addition, some studies reported the existence of groundwater in the Ko-Fuji volcano (Ikeda 1989; Nakai et al. 1995; Yasuhara et al. 2007; Gmati et al. 2011).

Hydrogeology in the southwestern area of Mt. Fuji

Figure 2 displays a geological map of the southwestern area of Mt. Fuji. Volcanic ejecta from the late Pleistocene to the Holocene are widely distributed on the slope area. The alluvial fan deposits of the Fuji River are distributed in lowland around the river. The Fuji River water comes from the Kofu basin, located at the north-west of Mt. Fuji. Other fan deposits distributed on the slope of Mt. Fuji (e.g. the deposit around well W12) are classified as volcanic fan deposits. Groundwater levels, obtained in 2013, showed that groundwater generally flows to the southwest and south. Although the existence of faults is known in the central part of the study area (Research Group for Active Faults of Japan 1991), hydrogeological characteristics of the surrounding area have not been clarified.

Geological cross sections through the slope to the coast, and from west to east, are shown in Fig. 3. There are six hydrogeological layers in the area (Murashita 1982), with an absence of a widely distributed impermeable layer. Layer A

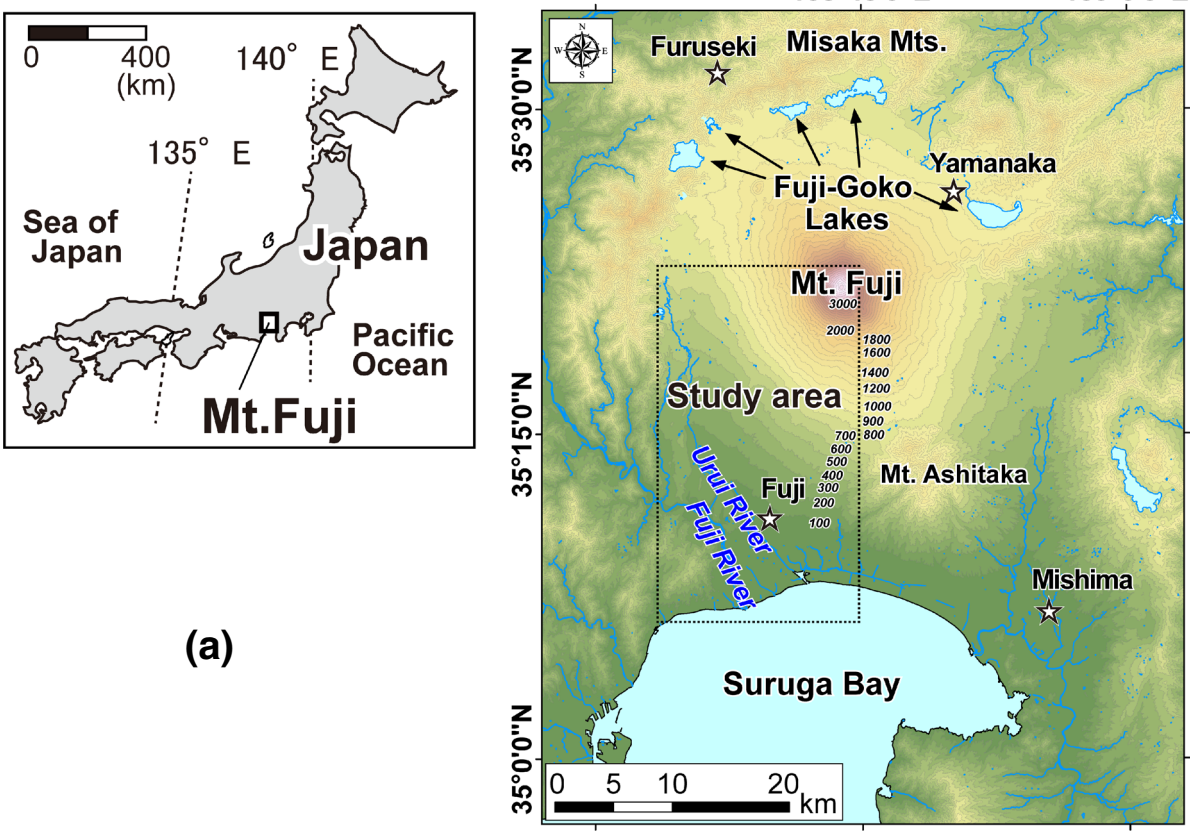

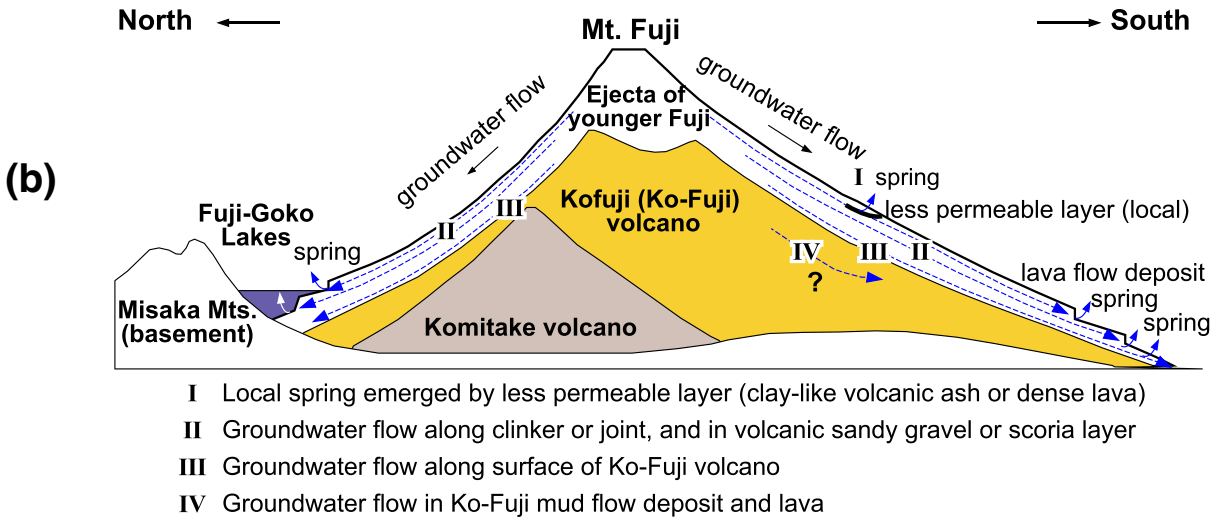

Fig. 1 **a** Location map of Mt. Fuji and study area; the solid white stars indicate the meteorological observatories of the Japan Meteorological Agency. The topographic map and river system were drawn using digital map data provided by the Geospatial Information Authority of Japan (2008). **b** Generalized geological model and groundwater flow system of Mt. Fuji (modified from Yasuhara et al. 2007)

(Fig. 3) is identical to Fuji River fan deposits in the lowland area (Fig. 2b). Layer B is basaltic lava associated with the ejecta of the younger Fuji (see Fig. 1b). In published papers, this lava deposit has been referred to by different names such as Fuji volcanic lava, New-Fuji lava, Shin-Fuji lava, or younger lava, depending on the authors. To be consistent with the description of "Ko-Fuji" volcano, the term of "Shin-Fuji" lava is used in this study. The lower part of the Shin-Fuji lava

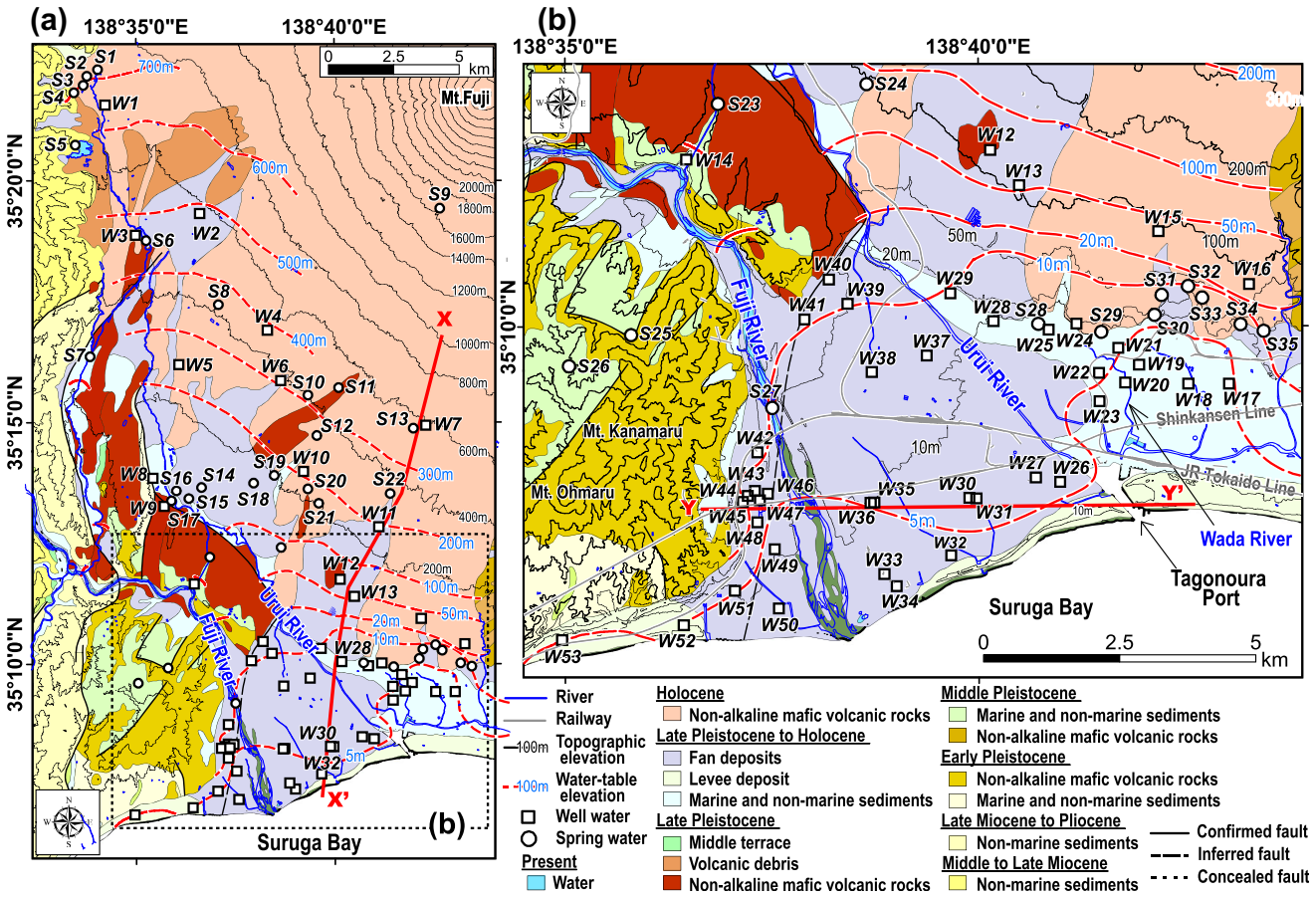

Fig. 2 **a** Surface geology, water-table elevation, and location of sampling sites in the study area. **b** Enlarged view of the lowland area. The surface geological map is from the digital seamless geological map (Geological Survey of Japan 2015). The water-table elevation was determined from observations in 2013 (Shizuoka Prefecture Government 2014). Well and spring specifications are shown in Tables S1 and S2 of the electronic supplementary material (ESM), respectively. The X–X′ and Y–Y′ cross sections are shown in Fig. 9a,b, respectively)

is permeable with many fissures, and the hydraulic conductivity ranges from 10^{-1} to 10^{-2} cm/s (Murashita 1982). The lava forms the main aquifer in the study area (Ikeda 1995) and is distributed in the coastal area with an inclination to the southwest (Fig. 3a; Murashita 1982).

Layer C consists of volcanic ash-mud, partially distributed in the lowland area (Fig. 3). Layer D, on the slope areas, is made up of volcanic ash, sand, and gravel layers, and is referred to as the Ko-Fuji mud-flow deposit, which erupted from the Ko-Fuji volcano (see Fig. 1b). The Ko-Fuji mud-flow deposit is basaltic composition and partially impermeable at the surface of the deposit (Ikeda 1995). However, groundwater in the Ko-Fuji volcano has been reported, as mentioned previously, and Gmati et al. (2011) suggested a vertical groundwater linkage through clinkers between the shallower Shin-Fuji lava and deeper Ko-Fuji aquifer. Although the time of deposition of the tuff breccia in the lowland (layer D) had not been clarified in the early 1980s (Murashita 1982), Ikeda (1989) mentioned that the Ko-Fuji mud-flow deposit underlies the Shin-Fuji lava in the coastal area.

Layer E is ejecta from the Ashitaka volcano and is distributed in the eastern part of the study area (Fig. 2b). The boundary between the lava of Mt. Fuji and the ejecta of Mt. Ashitaka coincides with the Wada River (Fig. 3a). The lowest layer (F) consists of sand and gravel layers similar to the material of layer A (Murashita 1982).

Methodology

Groundwater samples were collected at a total of 88 sites throughout the southwestern region of Mt. Fuji from November 2013 to January 2015 (Fig. 2). The specifications of the sampling sites, results of in-situ measurements, and chemical analyses are shown in Table S1 and Table S2 of the electronic supplementary material (ESM). Samples were collected from 50 wells, 3 artesian wells, and 35 natural springs. Duplicate sampling was carried out in 12 wells and 32 springs to determine seasonal fluctuations in chemical components in the study area. The first sampling was conducted in winter (November 2013) and the second sampling round was conducted during summer and autumn (July–October 2014).

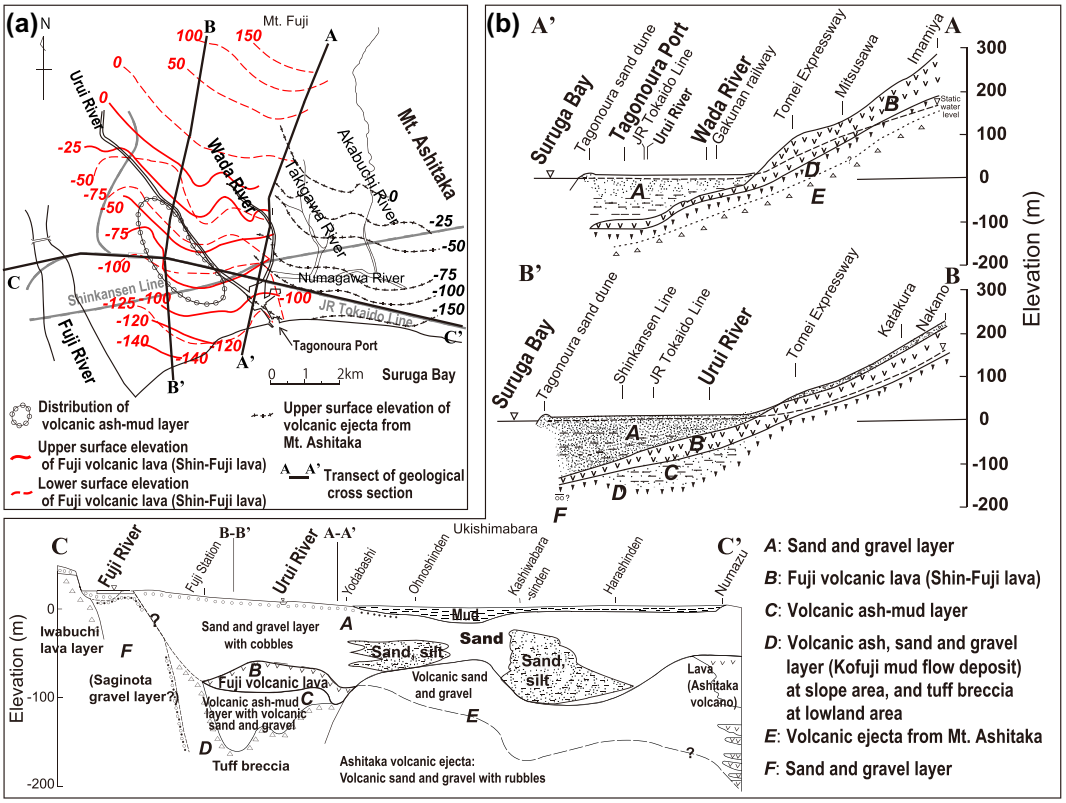

Fig. 3 **a** Map of the distribution of Fuji volcanic lava and ejecta from Mt. Ashitaka in the lowland. **b** Geological cross sections of A–A′, B–B′, and C–C′ (modified from Murashita 1982)

Water temperature, pH, electrical conductivity (EC), oxidation-reduction potential (ORP), and dissolved oxygen (DO) were measured in the field with portable meters (for EC: meter SC72, Yokogawa Electric Co., Japan; and D-54, HORIBA, Ltd., Japan; for pH, ORP, and DO: meters D-54, D-52, and D-55, HORIBA, Ltd., Japan, respectively). For sampling at the wells (except W3), groundwater was collected after stabilizing the physicochemical parameters (water temperature, pH, EC, ORP, and DO). Because the groundwater from W3 was temporarily stored in a tank and collected using a ladle, the ORP and DO measurements of the sample were excluded from the analysis. Natural spring water was collected directly with a tube from the mouth of the spring using the difference in hydraulic head. Where the hydraulic head was insufficient for sampling, a portable pump (CFC-a, Geo Science Lab, Japan) was used to collect the water. The in-situ ORP (E) was converted to a value of normal hydrogen electrode (E_{NHE}) using the equation $E_{NHE} = E + 206–0.7\ (t - 25)$ mV ($t = 0–60$ °C). The equation was provided by the operating manual of the portable meter D-52, manufactured by HORIBA, Ltd., Japan.

Alkalinity (pH 4.8) was determined using the 0.02 N H_2SO_4 titration method and was converted to a concentration of HCO_3^-. Water samples for the analysis of inorganic ions (Na^+, K^+, Mg^{2+}, Ca^{2+}, Cl^-, SO_4^{2-}, and NO_3^-) were first filtered using a 0.45-μm filter. The inorganic ion concentrations were analyzed using ion chromatography (Dionex ICS-5000, Thermo Scientific, USA) with analytical error of ±5%. The vanadium concentration, which is one of geochemical tracers used for elucidating rock–water interactions, was determined using ICP-MS (NexION 300, PerkinElmer, USA) after filtering water samples by using a 0.22-μm filter and adding nitric acid to lower the pH below 2. The error of vanadium analysis was ±8%.

Oxygen and hydrogen stable isotope ratios ($\delta^{18}O$, δD) were determined using a liquid water isotope analyzer (L2120-i, Picarro, USA) that employs a cavity ring-down spectrometer with analytical errors of ±0.2‰ for $\delta^{18}O$ and ±1‰ for δD. The values of $\delta^{18}O$ and δD were expressed relative to VSMOW (Vienna Standard Mean Ocean Water). Water samples collected for tritium (^3H) measurement were first distilled under reduced pressure using an automated evaporator (NVC2200 and N-2100, EYELA, Japan) before electrolytic accumulation of ^3H by an electrolysis instrument (Tori Pure, Permerec, Japan). Concentrations of ^3H in sampled water were determined using a liquid scintillation counter (AccuFLEX LSC-LB7, HITACHI ALOKA, Japan). Using this system, 0.3 tritium units (TU) could be quantified.

The data previously described, except for E_{NHE}, vanadium concentration observed in 2014, and ^3H concentration, had been reported as a data set of the water environment map developed by Ono et al. (2016). In this study, new investigations and results are presented with the additional data.

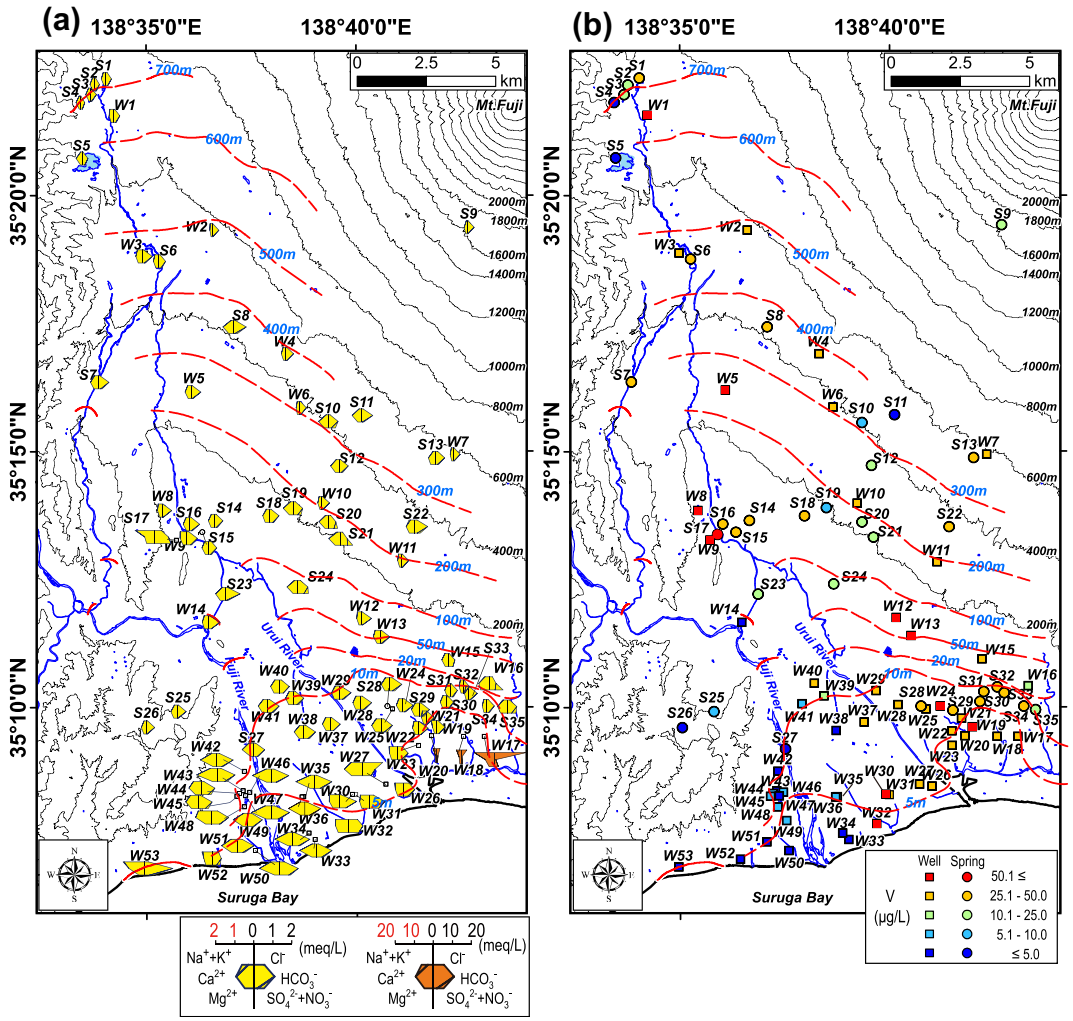

Fig. 4 **a** Stiff diagrams and **b** Vanadium concentrations in water samples for July 2014 to January 2015. (Red dashed lines represent the water-table elevation as shown in Fig. 2)

Results

Inorganic ions and vanadium concentrations in groundwater

The results of duplicate sampling from 2013 to 2014 are shown in Tables S1 and S2 of the ESM. These results showed that physicochemical parameters, inorganic ions concentrations, and isotopic compositions did not vary significantly in the sampling period. Therefore, geochemical analysis to determine the groundwater flow system for the study area was based on the results from July 2014 to January 2015 which cover the whole of the study area and contain tritium data.

Figure 4 shows the horizontal distribution of major ions using Stiff diagrams, and vanadium concentration in groundwater collected from July 2014 to January 2015. Figure 5 is a Piper plot of water samples from the study area. The Stiff diagrams showed that almost all of the groundwater samples were Ca-HCO_3 type; the well water close to the coast of Suruga Bay (e.g. W26, W33, W50, and W51) was Ca-HCO_3 type, and the well water from W32 was Na-HCO_3 type (Fig. 4). In contrast, well water in the eastern part of the study area (W17, W18, and W20) was Na-Cl type, with relatively high sodium and chloride concentrations, suggesting the mixing of freshwater and saltwater (Fig. 5). Spring water samples from S20, S21, S24, and S35 were characterized by high nitrate concentrations (Fig. 5).

The vanadium concentrations in groundwater ranged from 0.1 to 91.4 μg/L for the period from July 2014 to January 2015 (see Table S1 of the ESM). The concentrations were high for the slopes of Mt. Fuji and the lowland area around Urui River (Fig. 4b). By contrast, groundwater collected around the Fuji River had low vanadium concentrations.

Water temperature and isotopic composition in groundwater

Figure 6a shows the horizontal distribution of water temperature. Water temperature ranges from 9 to 22 °C (mean: 15 °C).

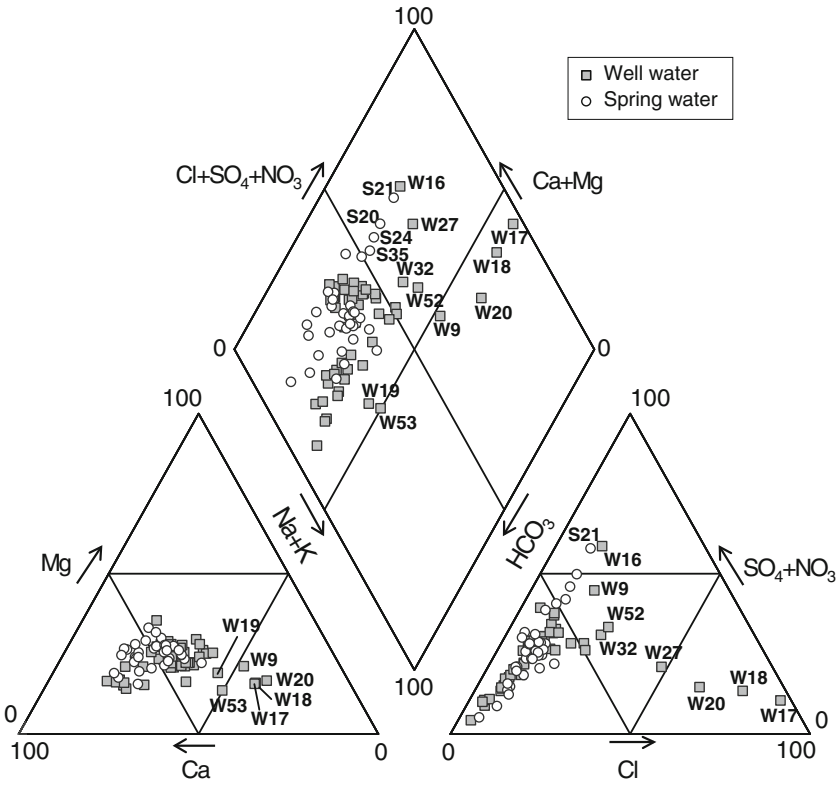

Fig. 5 Piper plot of water samples (collected from July 2014 to January 2015)

The lowest temperature was observed at spring S9, which is located at 1,633 m amsl. The inland springs (S1, S2, S3, S4, S5, and S6) also had relatively low temperatures. Well water samples collected on the slopes (W2, W3, W4, W6, W7, W10, and W11) and the lowland area (W19, W21, W22, and W24) had relatively low temperatures compared with the well water samples collected near Fuji River. The water temperatures near the coast at W30, W31, and W32 ranged from 14.1 to 15.2 °C, which was lower than those surroundings.

Figure 6b shows the horizontal distribution of δD in groundwater and Fig. 7 shows a delta diagram indicating the relationship between $\delta^{18}O$ and δD in water samples relative to meteoric water lines. The groundwater samples collected from July 2014 to January 2015 ranged from −7.0 to −10.8% for $\delta^{18}O$ and −43 to −74% for δD (Fig. 7). All of the groundwater samples plotted near the local and global meteoric water lines, indicating that the groundwater originated from meteoric water (Fig. 7).

The well water samples collected at higher elevations (W1, W2, and W7) had depleted δD values compared to those of samples collected at the foot of Mt. Fuji (W25, W28, W29, and W39; see Fig. 6b). In contrast, water samples from wells in the lowland (W16, W17, W45, W48, W52, and W53) had relatively enriched values of δD. The most notable aspect of the distribution of δD was observed in the coastal area of Suruga Bay: the deep wells W30, W31, and W32 (located close to the coast) showed depleted values of δD compared to wells away from the coast. The δD values of the wells closest to the coast ranged from −63 to −66% and were similar to values obtained for well water collected at high elevations (e.g. W1 and W2). The coastal groundwater was also characterized by high vanadium concentrations (Fig. 4b) and low water temperatures (Fig. 6a).

Discussion

Influence of anthropogenic activity on groundwater

Figure 4a shows that the well water samples at the eastern part of study area were grouped into Na-Cl type and the water table around those wells was lower than at the surrounding sites. In the 1960s, groundwater salinization occurred in the coastal area of Suruga Bay and saltwater was observed around Tagonoura Port area (Fig. 3a). Many hydrogeological investigations were carried out to reveal the salinization mechanism (Murashita and Kishi 1967; Murashita 1982; Ozaki 1978; Ikeda 1967, 1982, 1989, 1995). These studies concluded that groundwater salinization in the coastal area was mainly caused by sea water intrusion resulting from the over pumping of groundwater. In addition, the existence of a highly permeable volcanic aquifer in the coastal area permitted the rapid intrusion of sea water (Ikeda 1989, 1995). After a reduction in the pumping of groundwater in the area, water levels have

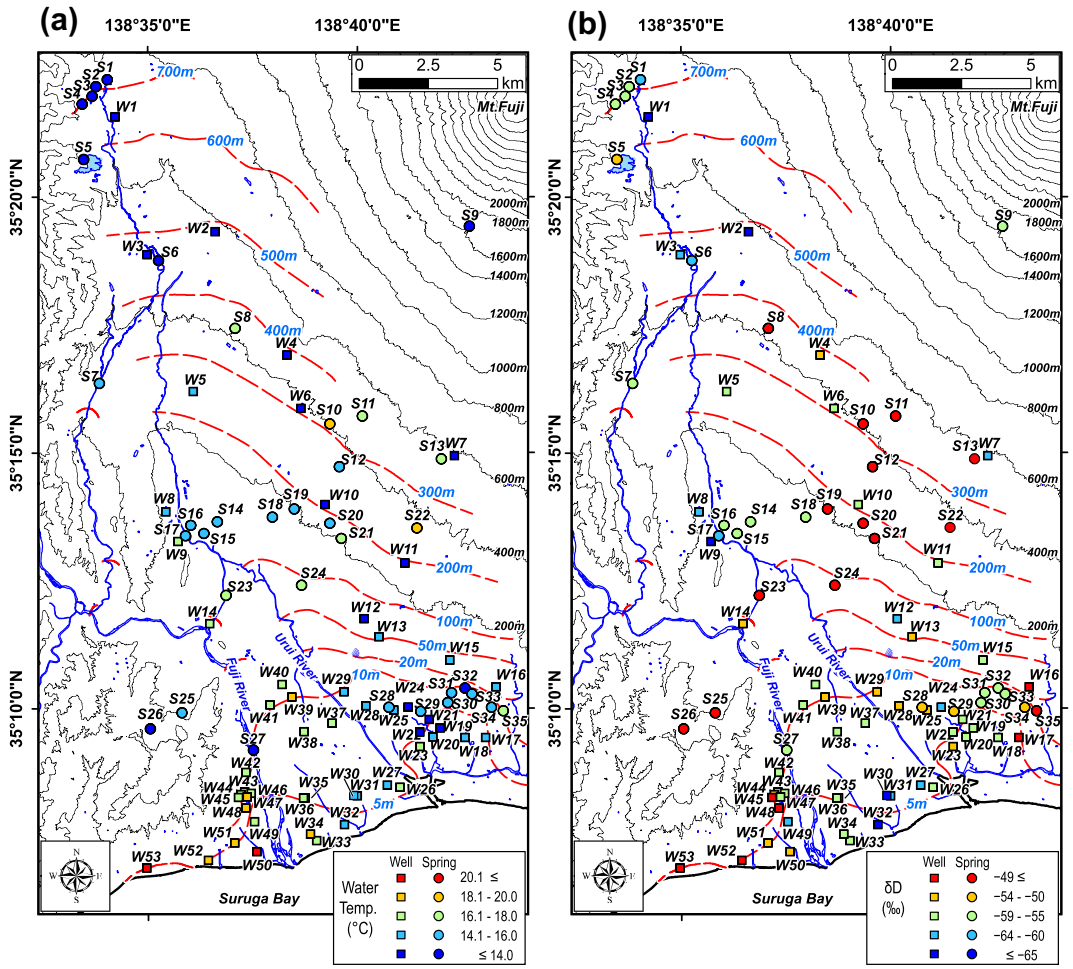

Fig. 6 **a** Water temperature and **b** δD in water samples for July 2014 to January 2015. (Red dashed lines represent the water-table elevation as shown in Fig. 2)

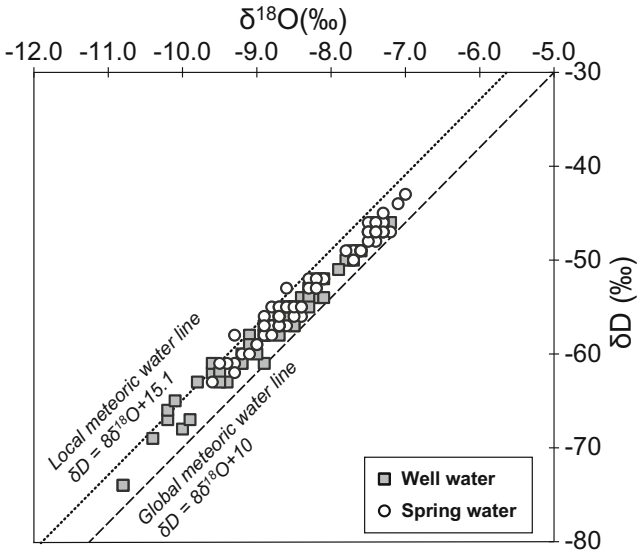

Fig. 7 Delta diagram of sampled water (collected from July 2014 to January 2015). The global meteoric water line is taken from Craig (1961), and the local meteoric water line is from Yasuhara et al. (2007)

risen and chloride concentrations have gradually decreased (Ikeda 1995). The present study included a sampling site with Na-Cl type water (W17, W18, and W20) and declining groundwater levels, suggesting that the influence of groundwater salinization has been retained.

The chemical characteristics of groundwater at the foot of Mt. Fuji and Mt. Ashitaka have recently been studied in detail (Shikazono et al. 2014; Kamitani et al. 2017). The studies grouped most of groundwater samples around the Mt. Fuji area into Ca-HCO_3 type, as done in this study. Shikazono et al. (2014) also investigated distributions of nitrate concentration and nitrogen isotopic composition in spring water. They found that high nitrate concentrations were derived from fertilizer use in agricultural areas around the mountains. In the current study, the spring water from S20, S21, S24, and S35 had high nitrate concentrations, which also suggest impacts from agricultural activity in the Mt. Ashitaka area. Thus, it can be concluded that the groundwater flow and the water quality in the eastern part of the study area have been disturbed by the anthropogenic activities more than in other parts.

Geochemical characteristics of groundwater derived from Mt. Fuji

To clarify the geochemical characteristics of groundwater derived from volcanic aquifers in Mt. Fuji, the study focused on vanadium concentrations and isotopic compositions. The vanadium concentration in groundwater has been investigated since the 1960s around the Mt. Fuji area and it was noticeably higher than in other watersheds in Japan (Okabe and Morinaga 1968; Okabe et al. 1981; Sakai et al. 1997). These studies suggested that the high vanadium concentration in groundwater was caused by dissolution from minerals in the basaltic Shin-Fuji lava. In contrast, the vanadium concentration in Fuji River water was less than 11 μg/L (Okabe and Morinaga 1968; Koshimizu and Kyotani 2002). Vanadium concentrations in the study area, therefore, can be used to identify the extent of groundwater derived from the basaltic aquifer of Mt. Fuji.

Figure 4b clearly shows that the groundwater derived from Mt. Fuji reaches the lowland around the Urui River and the coastal area where W30, W31, and W32 are located because the vanadium concentrations in those areas exceed 25 μg/L and are significantly higher than that of Fuji River water, as previously mentioned. In contrast, the well waters around Fuji River (e.g. W35, W38, W41) had low vanadium concentrations, similar to past Fuji River water (Okabe and Morinaga 1968). River levels observed at the Matsuoka observatory, which is located near S21, ranged from 10.3 to 14.2 m amsl in 2013 (Ministry of Land, Infrastructure, Transport and Tourism 2018); therefore, the water table observed in 2013 (Fig. 4b) showed that Fuji River water recharges the aquifer on its left (east) bank. Thus, Fuji River can be characterized as the influent river and well water with low vanadium concentration around the left bank of Fuji River should originate from river water. The distribution of vanadium concentrations also suggests that a boundary between groundwater with different recharge sources is located between W37 and W38, and between W30 and W36.

The isotopic composition of meteoric water and groundwater in the Mt. Fuji vicinity has also been thoroughly investigated (Yasuhara et al. 1997, 2007). Yasuhara et al. (1997) examined the characteristics of δD in rainfall from the slopes of Mt. Fuji and reported an altitude effect for which δD values are more depleted at higher elevations. The altitude effect of $\delta^{18}O$ was also described in Yasuhara et al. (2007). In addition, Yasuhara et al. (1997) postulated that evaporation had occurred before recharge took place and that a "recharge-water line" could be found by comparing discharge elevations of local springs and isotopic compositions of spring water. Unfortunately, the full formula for calculating the recharge water line was not given in Yasuhara et al. (1997), and therefore the recharge elevation (H) in this study was estimated using the equation $H = -50 \cdot \delta D - 1{,}200$, which was calculated from the read values of the graph in the paper (see Fig. S2 in the ESM).

Estimated recharge elevation includes ±50 m error based on the analytical error of δD. According to the equation, for example, a recharge elevation of spring S9, which is located at 1,633 m amsl and had a δD of −58%, was estimated at 1,700 m amsl. The result shows that the groundwater at S9 was recharged near the discharging point. Conversely, the δD values for coastal groundwater (W30 and W32) were −66 and −65%, respectively. It was estimated that the recharge elevation ranged from 2,100 to 2,050 m amsl. As there are no other mountains in the study area with high elevations except for Mt. Fuji, these greatly depleted values of δD in the coastal groundwater can be explained by higher recharge elevations on Mt. Fuji.

Vertical distribution of water temperature and isotopes at the lowland area

Vertical distributions of water temperature, δD, and ^{3}H concentrations are shown in Fig. 8. The figure shows data for wells at lower topographic elevations that correspond to groundwater levels of <100 m amsl; see Fig. 2b. The vertical distribution of water temperature (Fig. 8a,b) showed a tendency to decrease with depth, in contrast to the typical effect of the geothermal gradient (Freeze and Cherry 1979), which suggests that the geothermal gradient seems not to affect groundwater temperature in the study area strongly. Ikeda (1982) also reported a similar tendency in water temperatures at the foot of Mt. Fuji and concluded that groundwater recharged at higher elevations flows into the deep Ko-Fuji volcanic layer. The result implies that a large quantity of groundwater is recharged at high elevations and flows into Ko-Fuji volcano, and the large groundwater flow prevents the formation of the typical subsurface thermal structure. Another important observation was that both shallow and deep groundwater were under oxic conditions—e.g. W28 (18 m deep) and W22 (320 m deep), see Table S1 of the ESM, which suggests a huge flux of groundwater flow in Mt. Fuji because the consumption of oxygen is incomplete.

δD values of groundwater were depleted with increasing depth (Fig. 8c). In particular, the δD trend was clearly shown in the central part (from 138.64 to 138.68 °E) in the lowlands (Fig. 8d), suggesting that groundwater recharged at higher elevations reaches the coastal area of Suruga Bay after flowing through deeper parts of the area. This hypothesis is in agreement with the vertical distribution of water temperature, because water recharging at higher elevations must have a lower temperature than at lower elevations.

The relationships between ^{3}H concentration and elevation are shown in Fig. 8e,f. The ^{3}H concentrations measured in the shallower part (above −40 m amsl) of the study area ranged from 0.3 to 1.7 TU, suggesting that the groundwater residence time is relatively short. In contrast, ^{3}H was not detected in deeper groundwater (below −170 m amsl) as the residence time at these depths would be long. The concentrations of ^{3}H in the

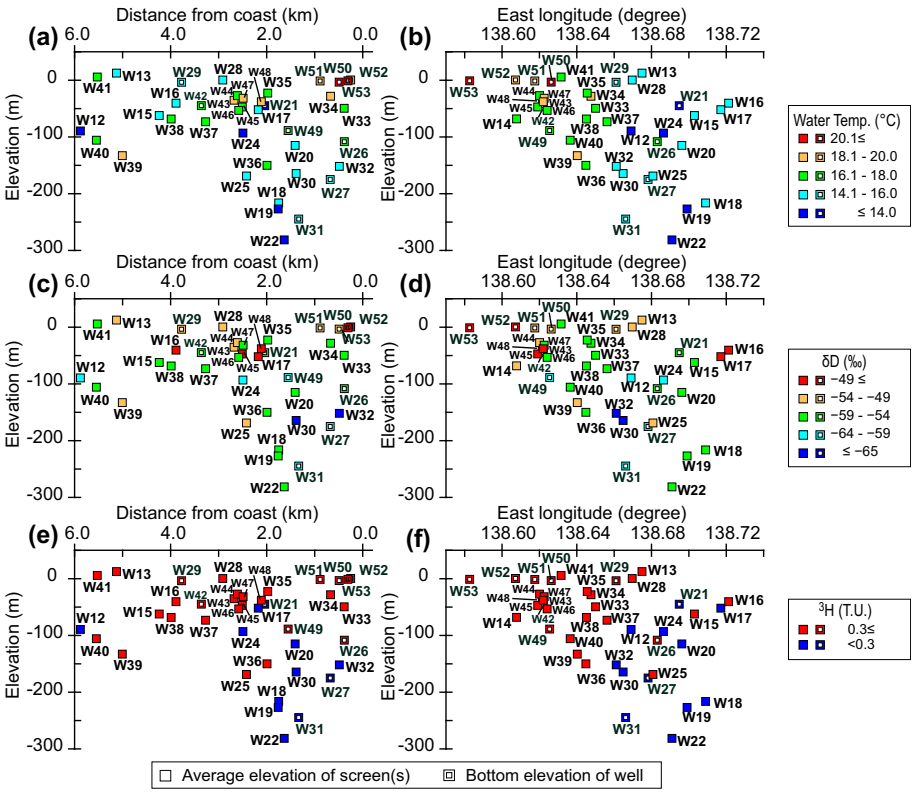

Fig. 8 Vertical distribution of observed water temperature and isotopic values in groundwater. The water temperature (**a**–**b**), δD (**c**–**d**), and ^{3}H concentration (**e**–**f**) are depicted by elevation versus the distance from the coast or the east longitude. Symbols are plotted by the average elevation of screen(s) or by the bottom elevation of the well in case of unknown screen depth

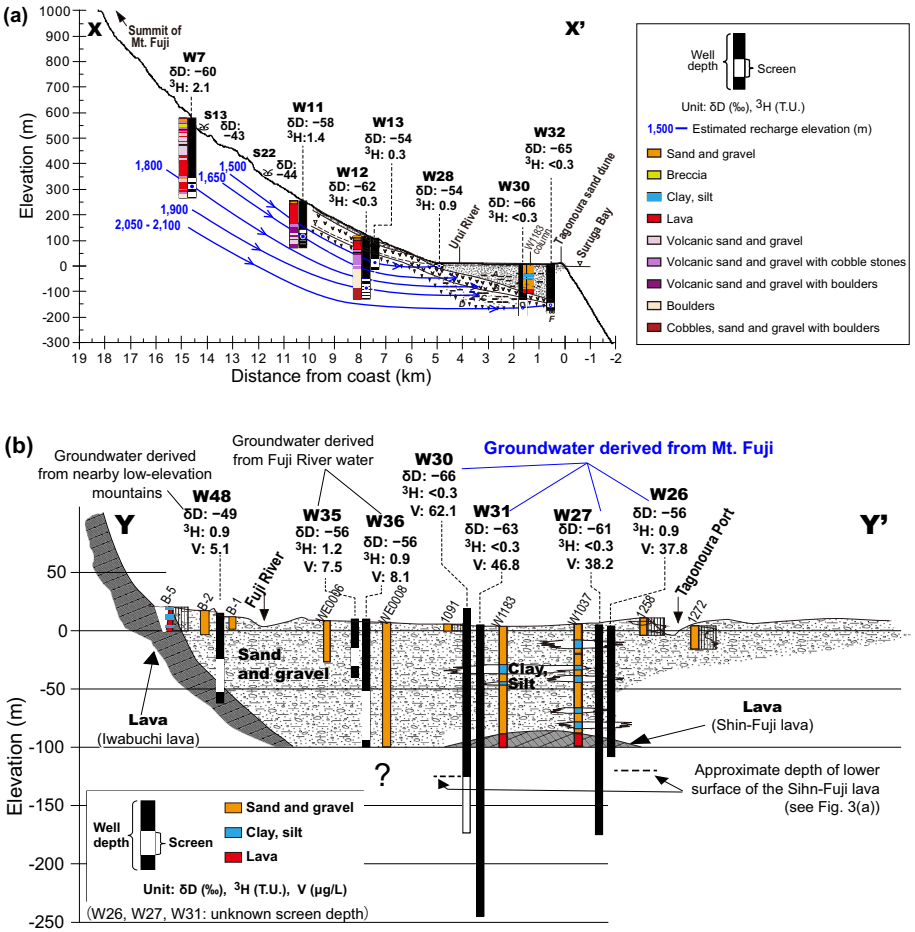

Fig. 9 **a** Cross section through the slope to the coast, showing the distribution of δD and ^{3}H concentrations with geology (the legend for layers A, B, C, and D is given in Fig. 3). **b** Cross section at the Y–Y′ transect showing the distribution of δD, ^{3}H, and vanadium concentrations. The geological cross section with log profiles was modified from Earthquake Preparedness Division, Shizuoka Prefecture Government (1984). Geological log profiles of W7, W11, W12, and W1183 are shown in detail in Fig. S1 of the ESM. The geochemical data illustrate the geochemical condition of groundwater around the screen or above the bottom of the well

intermediate zone (from −40 to −170 m amsl) ranged from less than 0.3 to 1.8 TU, suggesting that the residence time could have variable values. Consequently, the ^{3}H concentrations imply that the groundwater residence time in the deeper parts of the aquifer is generally longer than in the shallower parts.

Groundwater flow through the slope of Mt. Fuji to the coastal area of Suruga Bay

The horizontal distributions of vanadium concentration, water temperature, and δD in the study area (Figs. 4 and 6) suggest that coastal deep groundwater (e.g. W32) was recharged at higher elevations in Mt. Fuji and had high vanadium concentrations indicating the dissolution of vanadium from the basaltic aquifer of Mt. Fuji. In addition, the deep groundwater in the lowland was not noticeably affected by the geothermal gradient (Fig. 8a,b). To clarify the groundwater flow system through the slope area to the coastal area, the geology and isotope distributions were investigated along the X–X′ and Y–Y′ transects (Fig. 2a).

Figure 9a shows a cross section through the slope to the coast with well locations and screened depths. The geological cross section of B–B′, close to the X–X′ transect, was transposed into a cross section of X–X′ using the location of the river, railway lines, and elevations. To verify correspondence between the geological cross section of B–B′ and on-site geology, geological columns for sampling wells are depicted in the figure (the columns are shown in Fig. S1 of the ESM in detail). The geologic columns of sampled wells (W11 and W12) showed that the surface of the Ko-Fuji mud-flow deposit (layer D) approximately corresponds with the interface between the lava and the volcanic sand and gravel layer in the columns. The geology of column W1183 was consistent with the stratigraphy of the B–B′ cross section. The observed δD values of groundwater clearly show significant differences between shallower and deeper parts, implying that recharge elevations of those are different. Therefore, estimated recharge elevations based on the recharge-water line (Yasuhara et al. 1997) are depicted in Fig. 9a with assumed flow lines.

The recharge elevations of the coastal groundwater (wells W30 and W32) are higher than the recharge elevations of the slope-area groundwater (wells W7, W11, W12, and W13). In addition, the depth of coastal groundwater flow is deeper than the bottom depth of W12. The geological log of well W12 shows that the groundwater was collected from the layer of boulders, cobbles, sand, and gravel beneath the Ko-Fuji mud-flow deposit. Therefore, the coastal groundwater should be derived from aquifers in the Ko-Fuji volcano rather than the Shin-Fuji aquifer. The observed high vanadium concentrations in coastal groundwater (W30 and W32) might be caused by the dissolution of volcanic deposits from the Ko-Fuji volcano.

In contrast to the coastal groundwater, well water samples in the slope area (W7, W11, W12, and W13) had more enriched δD (−60, −58, −62, and −54‰, respectively) and the estimated recharge elevations of those ranged from 1,500 to 1,900 m. The groundwater represented by wells W7, W11, W12, and W13 flows in the upper part of Ko-Fuji mud-flow deposit (layer D). In addition, the groundwater should be recharging into aquifers of Shin-Fuji lava and fan deposits because well water in the lowland (e.g. W37) had a δD value of −55‰, which falls between −54‰ (W13) and −62‰ (W12). The δD values of springs S13 and S22 were largely enriched in comparison with those of wells W11 and W13; therefore, the spring water had the lowest recharge elevation in the cross section of X–X′ and it should flow in the Shin-Fuji lava. Thus, the δD results from the slope to the coast can be explained by a hierarchical groundwater flow system.

As with the results for δD, the ^{3}H concentrations in groundwater showed significant differences between the shallower and deeper parts. The ^{3}H concentrations of water samples from shallower parts, such as W7, W11, and W13, were more than 0.3 TU, implying that the residence time was relatively short. Conversely, the groundwater samples from deeper parts of the study area (W12, W30, and W32) had a lower ^{3}H content (< 0.3 TU), indicating that they have the longest residence time in the present study.

Figure 9b shows the cross section at the Y–Y′ transect, closest to the coast (see Fig. 2b). A significant difference in vanadium concentrations between the deep groundwater from W30 (200 m deep) and the shallow groundwater from W36 (110 m deep) was found, thus supporting the hypothesis of the presence of two different groundwater bodies on the left bank of Fuji River. Furthermore, Fig. 9b strongly suggested that the Fuji River water must migrate to an elevation of −94 m (the lower screen elevation of W36) at least, even if a large amount of groundwater comes from Mt. Fuji into this region. However, deep drilling in the coastal area is necessary to further unravel the hydrogeological environment in the deeper areas around the Fuji River. The groundwater from W48 on the right

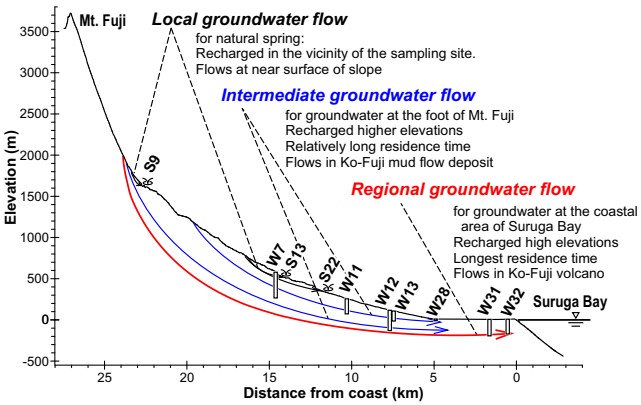

Fig. 10 Conceptual groundwater flow model through the slope of Mt. Fuji to the coastal area of Suruga Bay

bank of Fuji River had relatively enriched values of δD. The characteristics of the water table suggest that the groundwater at W48 originates from the low-elevation mountains near the sampling site (Mt. Ohmaru and Mt. Kanamaru; see Fig. 2b).

Conceptual model of the groundwater flow system of Mt. Fuji with the coastal area of Suruga Bay

Figure 10 shows a conceptual diagram of the groundwater flow system from Mt. Fuji to the coastal area of Suruga Bay. There are three patterns of groundwater flow. The natural springs such as S9, S13, and S22, were classified as "local groundwater flow". They can be recharged in the vicinity of the sampling sites S9, S13, and S22 and the groundwater flows in Shin-Fuji Lava at the slope area. The difference in elevation between the site of recharge and discharge is less than 1,000 m. Although, the ^{3}H concentration in spring water was not determined in the present study, a previous study reported that the groundwater age of a spring at the southwestern foot of Mt. Fuji ranged from 0 to 29 years (Tosaki et al. 2011); therefore, both the groundwater flow path and residence time should be short. The well waters distributed at the foot of Mt. Fuji (e.g. W13 and W28) were classified as "intermediate groundwater flow" and are characterized by recharging at higher elevations and having relatively long residence time. The groundwater flows in the upper part of Ko-Fuji mud-flow deposit and discharges at the foot of Mt. Fuji, some of which contributes to the recharging of the aquifers in Shin-Fuji lava and fan deposits in the lowland.

Coastal groundwater (e.g. W30 and W32) was considered to have a "regional groundwater flow" pattern. The coastal groundwater, which is recharged at high elevations and flows in the Ko-Fuji volcano, has the longest residence time in the study area. The groundwater is rarely affected by the geothermal gradient, and it therefore appears that very large quantities of groundwater flow into the Ko-Fuji volcano. To examine the residence times in the deeper parts, other age dating tracers such as ^{14}C and noble gas, should be used.

As shown Fig. 10, the groundwater flow system has a wide recharge zone (about 8 km in horizontal scale); furthermore, the groundwater flow reaches the coastal area, preventing the formation of a typical subsurface thermal structure (Fig. 8). These results suggest that very large quantities of groundwater flow inundate the coastal area; consequently, groundwater in the coastal area must be pushed strongly seaward. This condition can be confirmed by the spatial distribution of water quality, which shows that the Ca-HCO_3 type of groundwater with low salinity was found all over the study area even in deep groundwater very close to the coast (<2 km from the coast line). Additionally, the water from the influent river migrates to an elevation of −94 m (Fig. 9b), even if the large quantities of groundwater come from the volcano. Any impermeable layer has not been found at that elevation in the present study and, therefore, it seems that the active groundwater flow from Mt. Fuji prevents the migration of river water in the coastal area.

In steady-state groundwater flow modeling, the boundary condition at the shoreline is sometimes given as either a constant head or a no-flow boundary (Wang and Anderson 1982). While upward-rising groundwater flow should occur at the shoreline under the preceding conditions, the vertical distributions of δD and ^{3}H in the groundwater do not necessarily indicate strong upward flow (Fig. 7). In conclusion, one should use the boundary condition whereby (1) some groundwater flows upward and discharges into the coast, and (2) some must discharge directly at the sea floor at depths from 100 to 200 m.

Conclusions

Groundwater was investigated to elucidate the groundwater flow system from the slope area of Mt. Fuji to the coastal area of Suruga Bay by the spatially dense geochemical data. The horizontal distribution of isotopes, inorganic ions, vanadium, and water temperature revealed that the characteristics of groundwater derived from the volcanic aquifer of Mt. Fuji were different from that of groundwater in Mt. Ashitaka and Fuji River water. The groundwater recharged at higher elevation in Mt. Fuji has depleted in δD, which is explained by the altitude effect, and relatively high vanadium concentration as a result of the dissolution of basaltic lava. Those characteristics revealed the three patterns of groundwater flow as follows: (1) local groundwater flow represented by natural springs distributed on the slope areas of Mt. Fuji; (2) intermediate flow emerging as groundwater at the foot of Mt. Fuji, whereby some of the groundwater recharges aquifers of the Shin-Fuji lava and the lowland deposit; (3) regional groundwater flow in the Ko-Fuji volcano, reaching the coastal area of Suruga Bay. This geochemical investigation was conducted as an example of a stratovolcano adjacent to a coastal area with abundant groundwater, and it could help set the boundary condition for the discharge zone in numerical modeling of groundwater flow.

Acknowledgements The authors would like to express their appreciation to the local government of Shizuoka Prefecture, Fuji City, Fujinomiya City, Numazu City, and owners of the production wells for their cooperation with this investigation. The authors are most grateful to three reviewers and two editors for their useful comments and suggestions, which improved the manuscript considerably.

References

Asai K, Satake H, Tsujimura M (2009) Isotopic approach to understanding the groundwater flow system within an andesitic stratovolcano in a temperate humid region: case study of Ontake volcano, central Japan. Hydrol Process 23(4):559–571

Craig H (1961) Isotopic variations in meteoric waters. Science 133:1702–1703

Custodio E (1989) Groundwater characteristics and problems in volcanic rock terrains. In: IAEA (ed) Isotope techniques in the study of the hydrology of fractured and fissured rocks. Proceedings of an advisory group meeting, Vienna, 17–21 November 1986, pp 87–137

D'Alessandro W, Vita F (2003) Groundwater radon measurements in the Mt. Etna area. J Environ Radioact 65(2):187–201. https://doi.org/10.1016/S0265-931X(02)00096-6

Earthquake Preparedness Division, Shizuoka Prefecture Government (1984) Shizuoka Ken Chishitsu Danmenzu [Geological cross sections in Shizuoka Prefecture] (in Japanese). Countermeasure document for earthquakes, Earthquake Preparedness Division, Shizuoka, Japan

Ecker A (1976) Groundwater behavior in Tenerife, volcanic island (Canary Islands, Spain). J Hydrol 28(1):73–86. https://doi.org/10.1016/0022-1694(76)90053-6

Freeze RA, Cherry JA (1979) Groundwater. Prentice Hall, Upper Saddle River, NJ

Geological Survey of Japan, AIST (ed) (2015) Seamless digital geological map of Japan 1: 200,000. May 29, 2015 version. Geological Survey of Japan, National Institute of Advanced Industrial Science and Technology, Tsukuba, Japan

Geospatial Information Authority of Japan (2008) Fundamental geographical data. https://fgd.gsi.go.jp/download/info.html. Accessed 15 May 2015

Gmati S, Tase N, Tsujimura M, Tosaki Y (2011) Aquifers interaction in the southwestern foot of Mt. Fuji, Japan, examined through hydrochemistry and statistical analyses. Hydrol Res Lett 5:58–63. https://doi.org/10.3178/HRL.5.58

Heilweil VM, Solomon DK, Gingerich S, Verstraeten IM (2009) Oxygen, hydrogen, and helium isotopes for investigating groundwater systems of the Cape Verde Islands, West Africa. Hydrogeol J 17(5):1157–1174. https://doi.org/10.1007/s10040-009-0434-2

Herrera C, Custodio E (2008) Conceptual hydrogeological model of volcanic Easter Island (Chile) after chemical and isotopic surveys. Hydrogeol J 16(7):1329–1348. https://doi.org/10.1007/s10040-008-0316-z

Hildenbrand A, Marlin C, Conroy A, Gillot PY, Filly A, Massault M (2005) Isotopic approach of rainfall and groundwater circulation in the volcanic structure of Tahiti-Nui (French Polynesia). J Hydrol 302:187–208. https://doi.org/10.1016/j.jhydrol.2004.07.006

Ikeda K (1967) Study on salt water intrusion into ground water, part 2: geochemical research of salt ground water (in Japanese with English abstract). Bull Geol Surv Jpn 18(6):393–411

Ikeda K (1982) A study on chemical characteristics of ground water in Fuji area (in Japanese with English abstract). J Groundw Hydrol 24(2):77–93

Ikeda K (1989) Chemical evolution of groundwater quality in the southern foot of Mount Fuji. Bull Geol Surv Jpn 40(7):331–404

Ikeda K (1995) A hydrogeochemical study on the groundwater in the southern foot of Mt. Fuji: changes in the groundwater quality, related to hydrological changes before and after salinization of groundwater (in Japanese with English abstract). J Jpn Assoc Hydrol Sci 25(2):57–70

Japan Meteorological Agency (2015) Meteorological observation data from 1981 to 2010. http://www.jma.go.jp/jma/menu/menureport.html. Accessed 28 September 2015

Kamitani T, Watanabe M, Muranaka Y, Shin K, Nakano T (2017) Geographical characteristics and sources of dissolved ions of groundwater in the southern part of Mt. Fuji (in Japanese with English abstract). J Geogr 126(1):43–71

Kebede S, Travi Y, Asrat A, Alemayehu T, Ayenew T, Tessema Z (2008) Groundwater origin and flow along selected transects in Ethiopian rift volcanic aquifers. Hydrogeol J 16:55–73. https://doi.org/10.1007/s10040-007-0210-0

Kizawa T, Iida M, Matsuyama S, Miyawaki A (1969) Fujisan-Shizen no Nazo wo Toku- [Elucidation of the nature in Mt. Fuji]. NHK, Shibuya-ku, Japan

Koshimizu S, Kyotani T (2002) Geochemical behaviors of multi-elements in water samples from the Fuji and Sagami rivers, central Japan, using vanadium as an effective indicator (in Japanese with English abstract). Jpn J Limnol 63:113–124

Kurata N (1966) Hydrogeological map and explanatory text of the hydrogeology of Mt. Fuji, 1 :50,000 (in Japanese). Hydrogeol Maps Japan. 14:32

Macdonald GA, Abbott AT, Peterson FL (1983) Volcanoes in the sea: the geology of Hawaii, 2nd edn. University of Hawaii Press, Honolulu

Marui A, Yasuhara M, Kono T, Sato Y, Kakiuchi M, Hiyama T, Suzuki Y, Kitagawa M (1995) Water quality and Lake bottom springs of Lake Sai on Mt. Fuji's northern slope (in Japanese with English abstract). J Jpn Assoc Hydrol Sci 25(1):1–12

Meinzer OE (1930) Groundwater in the Hawaiian Islands. In: Geology and water resources of the Kau District, Hawaii. US Geol Surv Water Suppl Pap 616, 28 pp

Ministry of Land, Infrastructure, Transport and Tourism (2018) Water information system. http://www1.river.go.jp/. Accessed 16 April 2018

Mink JF (1976) Groundwater resources of Guam: occurrence and development. Technical report no. 1, Water Resources Research Center, University of Guam, Mangilao, Guam

Murashita T (1982) Salt-water intrusion into aquifers in Japan (in Japanese with English abstract). Bull Geol Surv Jpn 33(10):479–530

Murashita T, Kishi K (1967) Study on salt water intrusion into ground water, part 1: geohydrologic conditions of lava aquifer (in Japanese with English abstract). Bull Geol Surv Jpn 18(6):379–392

Nakai N, Kikuta N, Tsuchi R (1995) Isotopic composition of natural waters distributing around Mt. Fuji and its applications to hydrological study (in Japanese with English abstract). J Jpn Assoc Hydrol Sci 25(2):71–81

Okabe S, Morinaga T (1968) Vanadium and molybdenum in the river and estuary water which pour into the Suruga Bay, Japan (in Japanese). Nippon Kagaku Zassi 89(3):284–287

Okabe S, Sibasaki M, Oikawa T, Kawaguchi Y, Nihongi H (1981) Geochemical studies of spring and lakewaters on and around Mt. Fuji, vol 1 (in Japanese). J Fac Marine Sci Tokai Univ 14:81–105

Ono M, Ikawa R, Machida I, Marui A, Muranaka Y, Kamitani T, Oyama K, Ito A (2016) Water environment map, no.9: Mt. Fuji area (in Japanese). Geological Survey of Japan, Tsukuba, Japan

Ozaki T (1978) Sea water intrusion into confined water estimated from long-term observations of chloride ion contents, Fuji City, Shizuoka prefecture. Bull Geol Surv Jpn 29(10):645–666

Parisi S, Paternoster M, Kohfahl C, Pekdeger A, Meyer H, Hubberten HW, Spilotro G, Mongelli G (2011) Groundwater recharge areas of a volcanic aquifer system inferred from hydraulic, hydrogeochemical and stable isotope data: Mount Vulture, southern Italy. Hydrogeol J 19(1):133–153. https://doi.org/10.1007/s10040-010-0619-8

Prada SN, Silva MO, Cruz JV (2005) Groundwater behaviour in Madeira, volcanic island (Portugal). Hydrogeol J 13(5–6):800–812. https://doi.org/10.1007/s10040-005-0448-3

Research Group for Active Faults of Japan (ed) (1991) Shinpen Nihon no Katsudansou: Bunputzu to Siryo [Active faults in

Japan: distribution maps and materials (in Japanese). University of Tokyo Press, Tokyo

Sakai Y, Ohshita K, Koshimizu S, Tomura K (1997) Geochemical study of trace vanadium in water by preconcentrational neutron activation analysis. J Radioanal Nucl Chem 216(2):203–212

Scholl MA, Ingebritsen SE, Janik CJ, Kauahikaua JP (1996) Use of precipitation and ground water isotopes to interpret regional hydrology on a tropical volcanic island: Kilauea volcano area. Hawaii Water Resour Res 32(12):3525–3537. https://doi.org/10.1029/95WR02837

Shikazono N, Arakawa T, Nakano T (2014) Groundwater quality, flow, and nitrogen pollution at the southern foot of Mt. Fuji (in Japanese with English abstract). J Geogr 123(3):323–342. https://doi.org/10.5026/jgeography.123.323

Shizuoka Prefectural Government (2014) Heisei 25 Nendo Tobu Chiiki Chikasuimyaku Chyousa Gyoumu Itaku Houkokusyo [Report of groundwater investigation in eastern area of Shizuoka Prefecture in Heisei 25 fiscal year] (in Japanese). Report of Shizuoka Prefecture, Shizuoka, Japan

Stern HT, Macdonald GA (1947) Geology and ground-water resources of the island of Molokai, Hawaii. Bull 11, Hawaii Division of Hydrography, Honolulu

Tosaki Y, Tase N, Sasa K, Takahashi T, Nagashima Y (2011) Estimation of groundwater residence time using the ^{36}Cl bomb pulse. Groundwater 49(6):891–902

Tsuya H (1940) Geological and petrological studies of Volcano Fuji (in Japanese). J Geogr 52(8):347–361

Wang H, Anderson MP (1982) Introduction to groundwater modeling: finite difference and finite element methods, Academic, San Diego

Won JH, Lee JY, Kim JW, Koh GW (2006) Groundwater occurrence on Jeju Island, Korea. Hydrogeol J 14(4):532–547. https://doi.org/10.1007/s10040-005-0447-4

Yamamoto S (1970) Hydrologic study of volcano Fuji and its adjacent areas: a tentative approach to volcano hydrology (in Japanese with English abstract). Geogr Rev Jpn 43(5):267–284

Yasuhara M, Marui A, Kazahaya K (1997) Stable isotopic composition of groundwater from Mt. Yatsugatake and Mt. Fuji, Japan. Proc. of the Rabat Symp., IAHS Publ. 244, IAHS, Wallingford, UK, pp 335–344

Yasuhara M, Kazahaya K, Marui A (2007) An isotopic study on where, when, and how groundwater is recharged in Fuji volcano, central Japan (in Japanese with English abstract). In: Aramaki S, Fujii T, Nakada S, Miyaji N (eds) Fuji volcano. Yamanashi Institute of Environmental Sciences, Kofu, Japan, pp 389–405